

Translational energy spectra for single-electron capture by O^{2+} in He, Ne, and Ar

A. R. Lee,¹ A. C. R. Wilkins,² C. Leather,² and A. G. Brenton²

¹Physics Department, La Trobe University, Bundoora, Victoria 3083, Australia

²Mass Spectrometry Research Unit, University College of Swansea, Singleton Park, Swansea SA2 8PP, United Kingdom

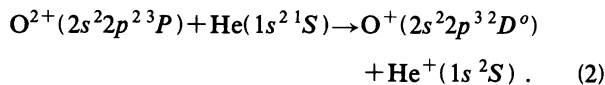
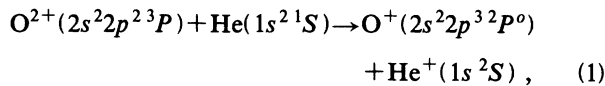
(Received 23 February 1994)

High-resolution single-electron capture spectra have been obtained for O^{2+} ions colliding with He, Ne, and Ar at 4-keV energy. For the He and Ne targets the dominant capture channels involve transitions from the ground 3P state of O^{2+} to the first and second excited states ($^2D^o$ and $^2P^o$) of O^+ . Eight well-resolved peaks are observed in each spectrum, corresponding to exactly the same capture channels with the target product ions (He^+ and Ne^+) undisturbed in their ground states. One relatively intense peak observed in the Ne spectrum is attributed to capture from the quintet state of O^{2+} ($2s2p^3^5S^o$) to the 4P state of O^+ ($2s2p^4^4P$). The O^{2+} in the Ar spectrum exhibits an entirely different character. Eight peaks are discernible, of which five are associated with capture channels which leave the target product Ar^+ ion in an excited state. The dominant channel is due to the ground-to-ground transition $O^{2+}(^3P) \rightarrow O^+(^4S^o)$ with the target Ar^+ ion formed in its first excited state ($3s3p^6^2S$).

PACS number(s): 32.70. - n

INTRODUCTION

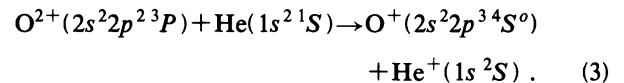
State-selective single-electron capture by O^{2+} in He has been the subject of considerable interest in recent theoretical [1–4] and experimental [5–7] studies. At collisions in the keV region, these spectra are dominated by two capture channels



The relative importance of these channels is at the center of current attention. The earlier calculations of Bienstock, Heil, and Dalgarno [3] predicted a predominance of the 2P capture channel for impact energies up to ~ 10 keV. While experiments at low energies (see Kamber *et al.* [6]) are in basic agreement, measurements at keV energies (McLaughlin *et al.* [5] and Kamber *et al.* [7]) contradict this expectation. The $^2D^o$ capture channel outweighs the $^2P^o$ channel at these higher experimental energies by a factor of ~ 2 . This prompted a theoretical reassessment by Bacchus-Montabonel, Courbin, and McCarroll [1] in which the adiabatic potential energies and relevant radial coupling matrix elements of the quasi-molecular system OHe^{2+} are calculated by *ab initio* methods, and interactions between $^3\Pi$ and $^3\Sigma$ states correlated to the initial and final channels are taken into consideration. Restriction to only triplet states correlated to the exit channels is justified since the entrance channel is a triplet state and spin conservation [8–10] prevents access to singlet states where the spin-orbit coupling is weak. This is evident in our present spectra for He. Their calculated ratios for the total capture cross sections $\sigma(^2D)/\sigma(^2P)$ in the energy range 125–500 eV/amu (2–8 keV for O^{2+} ions) are in good agreement

with previous experimental results [5,7]. Our intensity ratio of ~ 2.3 at 4 keV for the two capture channels [$O^{2+}(^3P) \rightarrow O^+(^2D)$]: [$O^{2+}(^3P) \rightarrow O^+(^2P)$] is somewhat higher than the calculated value of ~ 1.8 and previous experimental measurements. However, since our spectra are obtained from forward (small angle) scattering, the intensity ratios may be drastically affected by oscillations of the transfer probabilities with the impact parameter and may not be an accurate reflection of ratios of total cross sections. Inclusion of the $^3\Delta$ state for the 2D capture channel in the calculations may also boost the theoretical cross-section ratio, i.e., $\sigma(^2D)/\sigma(^2P)$.

Our spectrum for 4-keV O^{2+} in He reveals that the ground-to-ground capture channel is not entirely insignificant,



This peak is well resolved and amounts to $\sim 7\%$ of the intensity for capture into the $^2D^o$ state. Theoretical calculations would be valuable. Capture channels originating from the metastable $O^{2+}(2s^22p^2^1D)$ state have also been clearly identified.

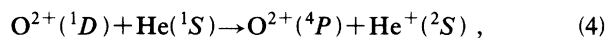
The spectrum for capture from the Ne target displays a very similar structure as that for the He target. The two capture channels corresponding to Eqs. (1) and (2) again predominate, but capture to the $^2P^o$ state is now three times more intense than for the $^2D^o$ state, reversing the tendency in He. An exceptionally intense peak has been identified for capture from the quintet state of $O^{2+}(2s^22p^3^5S^o)$ into the lowest quartet state of $O^+(2s2p^4^4P)$. The evidence is compelling. Capture from the ground 3P state of O^{2+} into the 4P state of O^{2+} is also significant at a mild endothermic energy change. These channels are apparent in the He spectrum as well, but at considerably lower intensities.

The spectrum for capture from the Ar target is unusual

in that it displays many capture channels in which the target product Ar^+ ion is formed in an excited state. The mechanism for charge transfer here is evidently different from that for the He and Ne targets, in that electrons in the target Ar atom appear to play an active role. Approximations based on configuration interaction calculations involving four outer electrons as assumed in the case of the O^{2+} -He complex [1] would not be adequate for this system. Conversely, a similar calculation for the O^{2+} -Ne complex could be illuminating.

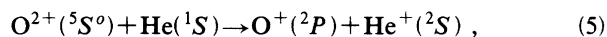
All 16 peaks observed in the spectra for capture in He and Ne targets are unambiguously identified with reaction channels, which satisfy the Wigner spin-conservation requirement [8–10].

The O^+ ion consists of a doublet-quartet spectroscopic system. Accordingly, all spectroscopic states in the O^+ ion are accessible to the ground-state $\text{O}^{2+}(^3P)$ ion by single-electron capture without violating spin conservation. Conversely, the singlet metastable 1D and 1S states of O^{2+} can only undergo transitions to the doublet (not quartet) states of O^+ by charge transfer. The following capture channel, for instance,

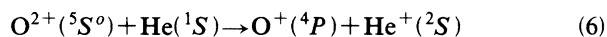


will obviously violate spin conservation.

Similarly, the doublet states of O^+ are not accessible to O^{2+} in the quintet $^5S^o$ state, e.g.,



violates spin conservation, whereas



satisfies the spin-conservation requirement.

Thus, the transition pattern for single-electron capture from the metastable 1D , 1S , and $^5S^o$ states of O^{2+} to O^+ will provide a viable test for spin-conservation studies. The observed absence of spin-forbidden channels in the transition pattern is an indication of the negligibility of spin-orbit interaction in the relevant collision systems. This appears to be the situation with capture from He and Ne. The correlation is less conclusive for capture by O^{2+} in Ar. There are three minor peaks attributed to spin-conserved transitions for which contributions from spin-forbidden processes with similar energy gains cannot be dismissed.

EXPERIMENT

The experimental results were obtained on a high-resolution translational energy loss spectrometer, described in detail elsewhere [11,12]. Briefly, O^{2+} ions were formed in a Nier-type combined electron-impact (EI)-chemical-ionization (CI) source operated in EI mode with 250-eV electrons and were accelerated to 4 keV. After mass selection through a magnetic sector, the ions pass through the first of two identical 90° electrostatic analyzers (ESA) and through a collision cell (2 mm in length). The energy loss spectrum is then produced by scanning in tandem the second ESA (90° deflection angle, 381-mm radius) and a smaller ESA (90° , 70-mm radius),

which is used to remove scattered ions from the walls and slits. Detection is by an off axis electron multiplier coupled to an electrometer. Only forward scattered (angular acceptance 0.015 rad in the plane of dispersion, 0.003 rad orthogonal to the plane of dispersion) O^+ ions are detected. The resolution of the precollisional ion beam was set at 0.2 eV. The collision gas was maintained at a pressure low enough to ensure single collisions dominated. All gases used were of research grade.

RESULTS AND DISCUSSION

The single-electron capture spectra for 4-keV O^{2+} in He, Ne, and Ar are shown in Figs. 1–3. Positive values of energy change refer to exothermic processes. We have adopted a slightly modified version of the notation used by Hasted and his co-workers (see Kamber, Mathur, and Hasted [13]) for convenient discussion of the capture processes. The designations I, II, III, . . . represent the ground and higher states of the incident ion (O^{2+} here); ordinary numerals 1, 2, 3, . . . represent the ground and higher states of the product in (O^+); and the Roman capital letters X, A, B, . . . represent the ground and successive excited states of the target product ion.

The spectrum for O^{2+} in He is shown in Fig. 1. In line with the conclusions of McLaughlin *et al.* [5] and Kamber *et al.* [7], the dominant peak E is identified with the I2X process for capture from the ground state of $\text{O}^{2+}(^3P)$ into the first excited state of $\text{O}^+(^2D^o)$, at a spectroscopic energy gain [15] of 7.25 eV and corresponding avoided crossing at $R_c = 3.7$ a.u. (dipole polarization of the ion-atom system having been neglected in this approximation),

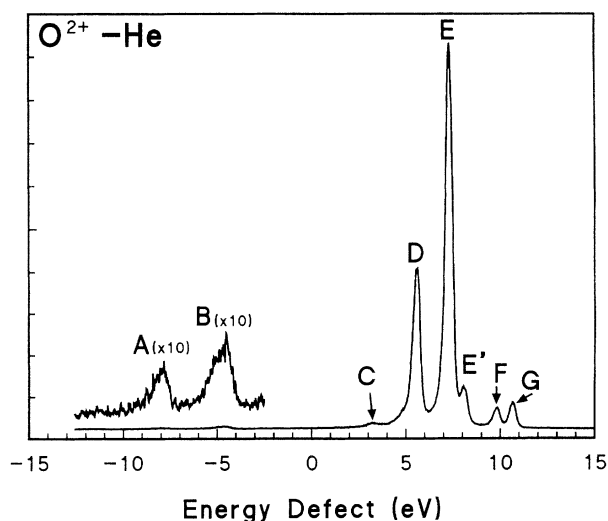
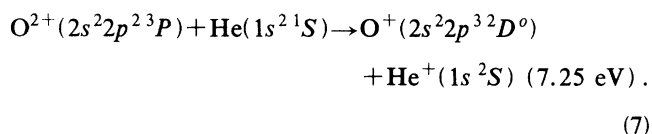


FIG. 1. Translational energy loss spectrum of O^+ resulting from single-electron capture by 4-keV O^{2+} ions in collision with He.

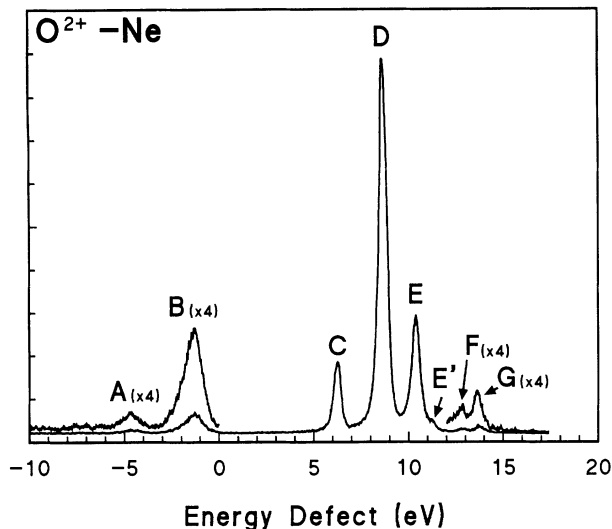


FIG. 2. Translational energy loss spectrum of O^+ resulting from single-electron capture by 4-keV O^{2+} ions in collision with Ne.

The next most prominent peak, D, measured at an energy gain of 5.5 eV, results from the I3X channel for capture from the ground state of $O^{2+}(2s^2 2p^2 \ ^3P)$ into the second excited state of $O^+(2s^2 2p^3 \ ^2P^o)$. This is also in agreement with previous identifications [5–7]. The observed capture channels are summarized in Table I(a).

The relatively well-resolved peaks F and G, measured at an energy gain of 9.7 and 10.5 eV are identified with the II2X and I1X channels, with peak heights of 5% and 7% respectively, relative to dominant peak E for the I2X process. The shoulder E', measured at an energy gain of 7.9 eV is identified with the II3X process. All these identified channels (D to G) involve capture by O^{2+} with

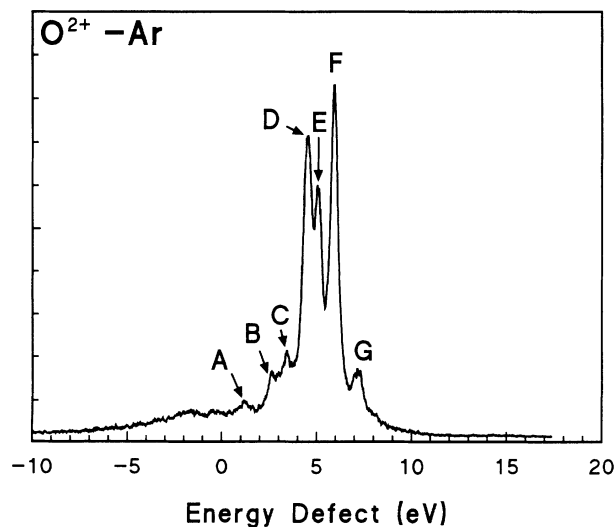
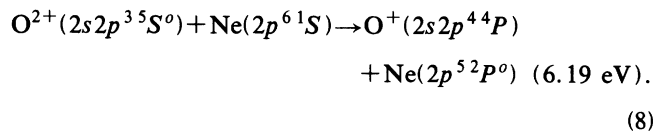


FIG. 3. Translational energy loss spectrum of O^+ resulting from single-electron capture by 4-keV O^{2+} ions in collision with Ar.

an electron configuration ($2s^2 2p^2$) into O^+ with a configuration ($2s^2 2p^3$). Contributions due to the IIX, II2X, and II3X processes have also been identified by McLaughlin *et al.* [5], although their II3X peak was not sufficiently resolved. Of the remaining weak structures, the barely perceptible peak C is interesting in that it may be identified with the IV4X process for capture from the quintet state of $O^{2+}(2s^2 2p^3 \ ^5S^o)$ into the lower quartet state of $O^+(2s^2 2p^4 \ ^4P)$. The identification here may not be very convincing, but the equivalent peak in the spectrum for O^{2+} in Ne (Fig. 2) is very prominent, and can be safely identified with the IV4X channel, as will be discussed later. It should be noted that the electron core is not disturbed in this transition. An electron is simply captured into a $2p$ orbital of the O^{2+} ion, leaving one $2s$ orbital unoccupied. Peaks A and B at endothermic energy changes are weak and relatively broad. Precise identification of the corresponding capture channels is difficult, but peak A may be due to the II5X process for the transition $O^{2+}(2s^2 2p^2 \ ^1D) \rightarrow O^+(2s^2 2p^4 \ ^2D)$, with capture accompanied by promotion of a $2s$ electron into a $2p$ orbital. The III7X and IV10X channels, with very similar energy gains, may also contribute to this peak. Core conservation is observed in these latter processes (see Table I). Peak B is probably due to the I4X channel for the transition $O^{2+}(2s^2 2p^2 \ ^3P) \rightarrow O^+(2s^2 2p^4 \ ^4P)$, which again involves capture with promotion of a $2s$ electron into a $2p$ orbital. The III5X channel may also contribute.

All the identified capture channels satisfy the spin-conservation requirements [8–10]. Spin-forbidden channels (such as II1X, II4X, III4X, and III6X) in the neighborhood of the observed channels are not apparent in the spectrum.

The capture spectrum for O^{2+} in Ne is shown in Fig. 2. The identified reaction channels for peaks A to G are summarized in Table I(b) and can be seen to correspond to exactly the same channels observed in the He spectrum. The I3X channel (peak D) is now dominant, with the I2X channel (peak E) next in intensity. These are the only two prominent transitions for the target, but in reverse order of prominence. For capture in Ne, there is a third substantial peak, C, measured at an energy gain of 6.0 eV. No capture channels originating from the ground 3P or first and second excited states (1D and 1S) of the O^{2+} ion have energy gains remotely close to this value, the spin nonconserved III4X transition being the nearest at 4.06 eV. However, the IV4X transition for $O^{2+}(2s^2 2p^3 \ ^5S^o) \rightarrow O^+(2s^2 2p^4 \ ^4P)$ is located at a spectroscopic energy gain of 6.19 eV, and must be identified with peak C,



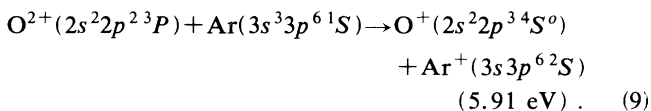
This transition entails the capture of an electron into a $2p$ orbital with one $2s$ orbital remaining vacant, and is clearly spin conserved. Capture from the quintet state of O^{2+} into a doublet state of O^+ would violate spin conservation. Such channels (e.g., IV3X and IV5X) are not ob-

TABLE I. Reaction channels for electron capture by 4-keV O^{2+} in (a) He, (b) Ne, and (c) Ar; the spectroscopic energy changes are determined from the compilations of Moore [15].

Peaks	Reaction channels	Designation	Measured energy gain (eV)	Spectroscopic energy (eV)	R_c (a.u.)	Peak height (%)
(a)						
A	$O^{2+}(2s^2 2p^2 \ ^1D) + He(1s^2 \ ^1S) \rightarrow O^+(2s 2p^4 \ ^2D) + He^+(1s^2 \ ^2S)$	II5X	-7.8	-7.50		< 1
	$O^{2+}(2s^2 2p^2 \ ^1S) + He(1s^2 \ ^1S) \rightarrow O^+(2s^2 2p^2 \ (^3P) 3s^2 \ ^2P) + He^+(1s^2 \ ^2S)$	III7X		-7.50		
	$O^{2+}(2s 2p^3 \ ^5S^o) + He(1s^2 \ ^1S) \rightarrow O^+(2s^2 2p^2 \ (^3P) 3p^4 \ ^4D) + He^+(1s^2 \ ^2S)$	IV10X	(?)	-7.59		
B	$O^{2+}(2s^2 2p^2 \ ^1P) + He(1s^2 \ ^1S) \rightarrow O^+(2s 2p^4 \ ^4P) + He(1s^2 \ ^2S)$	I4X	-4.5	-4.31		< 1
	$O^{2+}(2s^2 2p^2 \ ^1S) + He(1s^2 \ ^1S) \rightarrow O^+(2s 2p^4 \ ^2P) + He^+(1s^2 \ ^2S)$	III5X	(?)	-4.66		
C	$O^{2+}(2s^2 2p^3 \ ^3S^o) + He(1s^2 \ ^1S) \rightarrow O^+(2s 2p^4 \ ^4P) + He^+(1s^2 \ ^2S)$	IV4X	3.1	3.17	8.5	~2
D	$O^{2+}(2s^2 2p^2 \ ^3P) + He(1s^2 \ ^1S) \rightarrow O^+(2s^2 2p^3 \ ^2P^o) + He^+(1s^2 \ ^2S)$	I3X	5.5	5.55	4.9	43
E	$O^{2+}(2s^2 2p^2 \ ^3P) + He(1s^2 \ ^1S) \rightarrow O^+(2s^2 2p^3 \ ^2D^o) + He^+(1s^2 \ ^2S)$	I2X	7.3	7.25	3.7	100
E'	$O^{2+}(2s^2 2p^2 \ ^1D) + He(1s^2 \ ^1S) \rightarrow O^+(2s^2 2p^3 \ ^2P^o) + He^+(1s^2 \ ^2S)$	II3X	7.9	8.05	3.4	~11
F	$O^{2+}(2s^2 2p^2 \ ^1D) + He(1s^2 \ ^1S) \rightarrow O^+(2s^2 2p^3 \ ^2D^o) + He^+(1s^2 \ ^2S)$	II2X	9.7	9.76	2.8	5
G	$O^{2+}(2s^2 2p^2 \ ^2P) + He(1s^2 \ ^1S) \rightarrow O^+(2s^2 2p^3 \ ^4S^o) + He^+(1s^2 \ ^2S)$	I1X	10.5	10.57	2.6	7
(b)						
A	$O^{2+}(2s^2 2p^2 \ ^1D) + Ne(2p^6 \ ^1S) \rightarrow O^+(2s 2p^4 \ ^2D) + Ne^+(2p^5 \ ^2P^o)$	II5X	-4.6	-4.48		~1
	$O^{2+}(2s^2 2p^2 \ ^1S) + Ne(2p^6 \ ^1S) \rightarrow O^+(2s^2 2p^2 \ (^3P) 3s^2 \ ^2P) + Ne^+(2p^5 \ ^2P^o)$	III7X		-4.48		
	$O^{2+}(2s 2p^3 \ ^5S^o) + Ne(2p^6 \ ^1S) \rightarrow O^+(2s^2 2p^2 \ (^3P) 3p^4 \ ^4D) + Ne^+(2p^5 \ ^2P^o)$	IV10X	(?)	-4.57		
B	$O^{2+}(2s^2 2p^2 \ ^3P) + Ne(2p^6 \ ^1S) \rightarrow O^+(2s 2p^4 \ ^4P) + Ne^+(2p^5 \ ^2P^o)$	I4X	-1.3	-1.29		6
C	$O^{2+}(2s 2p^3 \ ^5S^o) + Ne(2p^6 \ ^1S) \rightarrow O^+(2s 2p^4 \ ^4P) + Ne^+(2p^5 \ ^2P^o)$	IV4X	6.0	6.19	4.4	19
D	$O^{2+}(2s^2 2p^2 \ ^3P) + Ne(2p^6 \ ^1S) \rightarrow O^+(2s^2 2p^3 \ ^2P^o) + Ne^+(2p^5 \ ^2P^o)$	I3X	8.6	8.57	3.2	100
E	$O^{2+}(2s^2 2p^2 \ ^3P) + Ne(2p^6 \ ^1S) \rightarrow O^+(2s^2 2p^3 \ ^2D^o) + Ne^+(2p^5 \ ^2P^o)$	I2X	10.4	10.27	2.6	31
E'	$O^{2+}(2s^2 2p^2 \ ^1D) + Ne(2p^6 \ ^1S) \rightarrow O^+(2s^2 2p^3 \ ^2P^o) + Ne^+(2p^5 \ ^2P^o)$	II3X	11.4	11.22	2.4	
F	$O^{2+}(2s^2 2p^2 \ ^1D) + Ne(2p^6 \ ^1S) \rightarrow O^+(2s^2 2p^3 \ ^2D^o) + Ne^+(2p^5 \ ^2P^o)$	II2X	12.9	12.78	2.1	1
G	$O^{2+}(2s^2 2p^2 \ ^3P) + Ne(2p^6 \ ^1S) \rightarrow O^+(2s^2 2p^3 \ ^4S^o) + Ne^+(2p^5 \ ^2P^o)$	I1X	13.6	13.57	2.0	2
(c)						
A	$O^{2+}(2s^2 2p^2 \ ^1D) + Ar(3s^2 3p^6 \ ^1S) \rightarrow O^+(2s 2p^4 \ ^2D) + Ar^+(3p^5 \ ^2P^o)$	II5X	1.2	1.32	22	~10
	$O^{2+}(2s^2 2p^2 \ ^1S) + Ar(3s^2 3p^6 \ ^1S) \rightarrow O^+(2s^2 2p^2 \ (^3P) 3s^2 \ ^2P) + Ar^+(3p^5 \ ^2P^o)$	III7X		1.32		
B	$O^{2+}(2s^2 2p^2 \ ^3P) + Ar(3s^2 3p^6 \ ^1S) \rightarrow O^+(2s^2 2p^3 \ ^2D^o) + Ar^+(3s 3p^6 \ ^2S)$	I2A	2.7	2.59	10.5	~18
	$O^{2+}(2s^2 2p^3 \ ^5S^o) + Ar(3s^2 3p^6 \ ^1S) \rightarrow O^+(2s 2p^4 \ ^2S) + Ar^+(3p^5 \ ^2P^o)$	IV8X(SV)		2.60		
C	$O^{2+}(2s^2 2p^2 \ ^1D) + Ar(3s^2 3p^6 \ ^1S) \rightarrow O^+(2s^2 2p^3 \ ^2P^o) + Ar^+(3s 3p^6 \ ^2S)$	II3A	3.5	3.40	8.0	~24
	$O^{2+}(2s 2p^3 \ ^5S^o) + Ar(3s^2 3p^6 \ ^1S) \rightarrow O^+(2s^2 2p^2 \ (^3P) 3s^2 \ ^2P) + Ar^+(3p^5 \ ^2P^o)$	IV7X(SV)		3.45		
D	$O^{2+}(2s^2 2p^2 \ ^3P) + Ar(3s^2 3p^6 \ ^1S) \rightarrow O^+(2s^2 2p^4 \ ^4P) + Ar^+(3p^5 \ ^2P^o)$	I4X	4.4	4.51	6.0	85
E	$O^{2+}(2s^2 2p^2 \ ^1D) + Ar(3s^2 3p^6 \ ^1S) \rightarrow O^+(2s^2 2p^3 \ ^2D^o) + Ar^+(3s 3p^6 \ ^2S)$	II2A	5.0	5.10	5.3	71
F	$O^{2+}(2s^2 2p^2 \ ^3P) + Ar(3s^2 3p^6 \ ^1S) \rightarrow O^+(2s^2 2p^3 \ ^4S^o) + Ar^+(3s 3p^6 \ ^2S)$	I1A	5.9	5.91	4.6	100
G	$O^{2+}(2s 2p^3 \ ^5S^o) + Ar(3s^2 3p^6 \ ^1S) \rightarrow O^+(2s^2 2p^3 \ ^2D^o) + Ar^+(3s^2 3p^4 \ (^3P) 3d^4 \ ^4D)$	IV2B	7.2	7.15	3.8	~19
	$O^{2+}(2s^2 2p^2 \ ^1D) + Ar(3s^2 3p^6 \ ^1S) \rightarrow O^+(2s^2 2p^4 \ ^4P) + Ar^+(3p^5 \ ^2P^o)$	II4X(SV)		7.02	3.9	

served in this spectrum.

While the spectrum for O^{2+} in He and Ne targets are well resolved and the peaks A to G span a wide energy range of ~18 eV covering endothermic to exothermic channels, the eight peaks (A to G) observed in the spectrum for O^{2+} in Ar (Fig. 3) are bunched in an exothermic energy range of only 6 eV. The dominant peak F is identified with the I1A channel in which a 2s electron is captured from the target Ar atom by the $O^{2+}(2s^2 2p^2 \ ^3P)$ ion in its ground state into $O^+(2s^2 2p^3 \ ^4S^o)$, also in its ground state. The target product ion is thus kept in the first excited state of $Ar^+(3s 3p^6 \ ^2S)$,



Single-electron capture processes in which the target product ion is formed in an excited state is seldom observed to any appreciable extent. One that dominates a given spectrum is certainly unusual. This capture channel is favored by the curve-crossing distance of 4.6 a.u., but it is not immediately apparent when the I4X process is the only prominent channel (peak D) in this spectrum in which the product target Ar^+ ion is formed in the ground state.

The other prominent peak, E, is associated with the II2A process for capture from the first excited state of $O^{2+}(2s^2 2p^3 \ ^2D^o)$, again with the Ar^+ ion in its first excited state. Of the remaining minor peaks, B and C are identified with the I2A and II3A channels; the spin-nonconserved channels IV8X and IV7X with nearby energy gains are also listed in Table I(c), but are considered

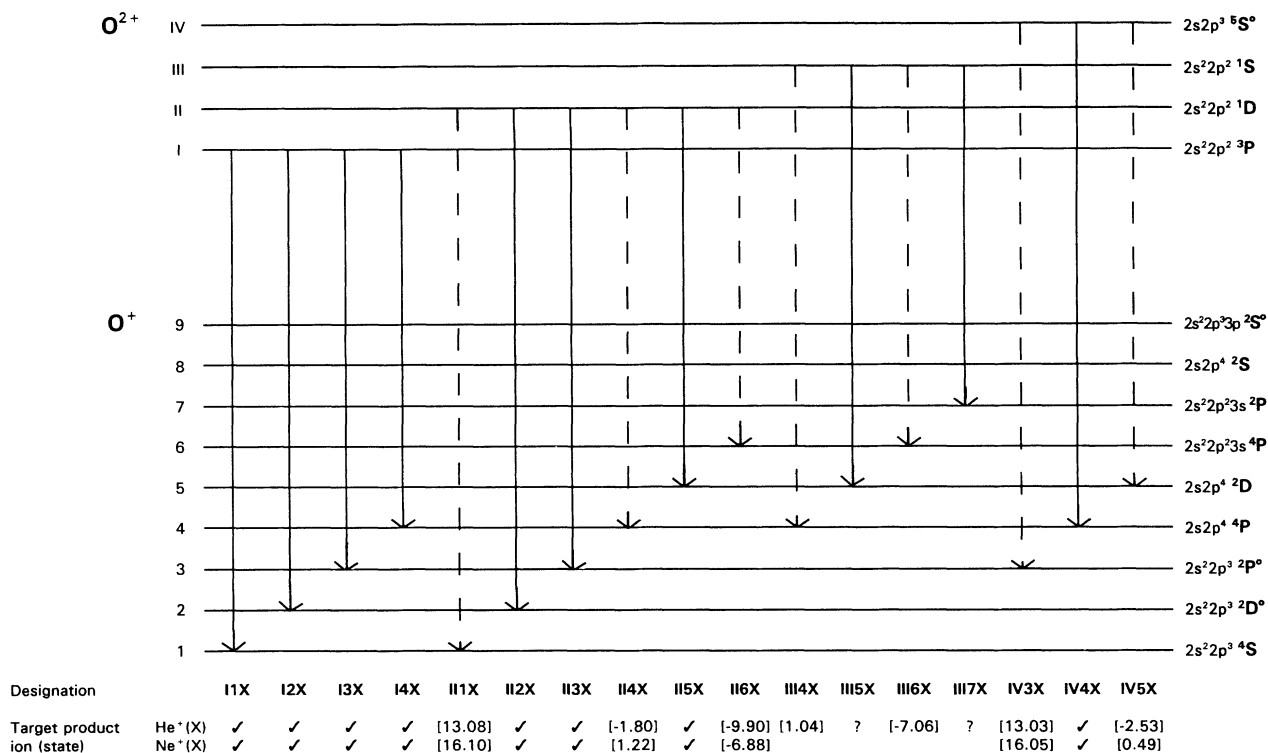


FIG. 4. Transition diagram for single-electron capture of 4-keV O^{2+} ions from He and Ne. Only the transitions in which the target remains in the ground state (X) are shown.

unlikely participants.

Peak G, measured at an energy gain of 7.2 eV, is speculatively identified with the unusual IV2B process, which involves capture from the quintet state of $O^{2+}(2s2p^3\ ^5S^o)$ with the target product ion formed in its second excited state $Ar^+(3s^23p^4(^3P)3d\ ^4D)$. This process is spin conserved, but the spin-nonconserved II4X channel at spectroscopic energy gain of 7.02 eV may also be considered a viable alternative.

The identified reaction channels for single-electron capture by 4-keV O^{2+} in He, Ne, and Ar are shown in Table I, with channel designations also given. SV after these designations indicates spin violation. The curve-crossing distances R_c are only approximate, with dipole polarization of the ion-atom systems neglected. The relative peak heights are normalized to 100% for the strongest peak observed in the respective spectra. Peak heights enclosed in brackets signify that the relevant peaks are not sufficiently resolved from the raised background.

A transition diagram for spin conserved and disallowed transitions is shown in Fig. 4. A similar diagram has been used in our previous study [14] of spin conservation for the capture processes involving $N^{2+} \rightarrow N^+$. The energy levels are symbolically represented by horizontal lines (labeled I, II, III, IV, . . . for O^{2+} and 1, 2, 3, . . . , 9, . . . for O^+). Transitions are represented by vertical lines; solid lines for spin-allowed transitions, and broken lines for spin-forbidden transitions. The bottom rows represent the target product ion (and their states X, A, B, . . .). Only the ground state X is involved in these transitions for O^{2+} in He and Ne. A check mark in the target row indicates observed channels; a question mark

indicates a tentative assignment and numbers in parentheses correspond to the spectroscopic values of energy changes (in eV) for the disallowed transitions, absent in the observed spectra. Negative energies indicate endothermic processes. The display affords easy detection of absent competing reaction channels in the vicinity of observed transitions. Spin-nonconserved transitions are conspicuously absent.

CONCLUSION

Single-electron capture by 4-keV O^{2+} in He is predominated by the capture channel $O^{2+}(^3P) \rightarrow O^+(^2D)$ in preference to capture into $O^+(^2P)$, in general agreement with recent theoretical prediction and experimental results. Capture into $O^+(^4S)$ is also significant in our well-resolved spectrum for O^{2+} in He. The spectrum for Ne target reveals similar features except for the notable dominance of the capture channel $O^{2+}(^3P) \rightarrow O^+(^2P)$ over that for $O^{2+}(^3P) \rightarrow O^+(^2D)$ by a factor of 3. A relatively intense peak is also observed for the unusual capture channel $O^{2+}(^5S^o) \rightarrow O^+(^4P)$ in the Ne target. All observed channels for capture in He and Ne are spin conserved. The spectrum for O^{2+} in Ar displays distinctly different features, with a predominance of capture channels, which involve formation of the target Ar^+ ion in an excited state.

ACKNOWLEDGMENTS

A.C.R.W. and C.L. thank the Engineering and Physical Sciences Research Council for financial support.

- [1] M. C. Bacchus-Montabonel, C. Courbin, and R. McCarroll, *J. Phys. B* **24**, 4409 (1991).
- [2] M. Gargaud, M. C. Bacchus-Montabonel, and R. McCarroll, *J. Chem. Phys.* **99**, 4495 (1993).
- [3] S. Bienstock, T. G. Heil, and A. Dalgarno, *Phys. Rev. A* **29**, 503 (1984).
- [4] S. E. Butler, T. G. Heil, and A. Dalgarno, *J. Chem. Phys.* **80**, 4986 (1984).
- [5] T. K. McLaughlin, S. M. Wilson, R. W. McCullough, and H. B. Gilbody, *J. Phys. B* **23**, 737 (1990).
- [6] E. Y. Kamber, C. L. Cooke, J. P. Giese, J. O. K. Pedersen, and W. Waggoner, *Phys. Rev. A* **36**, 5575 (1987).
- [7] E. Y. Kamber, A. G. Brenton, J. H. Beynon, and J. B. Hasted, *J. Phys. B* **18**, 933 (1985).
- [8] E. Wigner, *Nachr. Akad. Wiss. Goettingen Math. Phys. Kl. 2A*, 375 (1927).
- [9] A. R. Lee, C. S. Enos, and A. G. Brenton, *Int. J. Mass Spectrom. Ion Processes* **104**, 137 (1991).
- [10] A. R. Lee, C. S. Enos, and A. G. Brenton, *J. Chem. Phys.* **94**, 6017 (1991).
- [11] J. H. Beynon, A. G. Brenton, and L. C. E. Taylor, *Int. J. Mass Spectrom. Ion Processes* **64**, 239 (1985).
- [12] P. Jonathan, M. Hamdan, A. G. Brenton, and G. D. Willett, *Chem. Phys.* **119**, 159 (1988).
- [13] E. Y. Kamber, D. Mathur, and J. B. Hasted, *J. Phys. B* **15**, 263 (1982).
- [14] A. R. Lee, A. C. R. Wilkins, C. S. Enos, and A. G. Brenton, *Phys. Rev. A* **48**, 2934 (1993).
- [15] C. E. Moore, *Atomic Energy Levels*, Natl. Bur. Stand. (U.S.) Circ. No. 467 (U.S. GPO, Washington, DC, 1949).